

Received September 15, 2021, accepted September 29, 2021, date of publication October 4, 2021, date of current version October 11, 2021.

Digital Object Identifier 10.1109/ACCESS.2021.3117570

Generating Infinitely Many Coexisting Attractors via a New 3D Cosine System and Its Application in Image Encryption

BING LIU¹, XIAOLIN YE¹, (Graduate Student Member, IEEE), AND QIANQIAN CHEN²

¹School of Mathematics and Information Sciences, Anshan Normal University, Anshan 114007, China

²College of Electrical Engineering, Dalian University of Science and Technology, Dalian 116052, China

Corresponding author: Xiaolin Ye (yexl@dlmu.edu.cn)

This work was supported in part by the National Natural Science Foundation of China under Grant 12171004, and in part by the Natural Science Foundation of Liaoning Province under Grant 20170540001.

ABSTRACT In this paper, a new third-order chaotic system which has extremely multistability is constructed by introducing the boosted control of cosine function. In comparison with other chaotic systems of extremely multistability, the proposed chaotic system can spontaneously generate the infinitely many coexisting attractors towards two directions of the phase plane. It indicates the proposed system can output more chaotic sequences of different amplitudes at the same time. This peculiar physical phenomena is very interesting and worth studying. Relative to original chaotic system, the chaos characteristic of the proposed system is obviously enhanced, the value of max Lyapunov exponent is increased significantly and the complexity value was higher. In particular, many periodic windows of the original chaotic system become chaos. It means the proposed chaotic system has better chaotic characteristics. If the new system is applied to the field of cryptography, it would be a better system model as a pseudo-random signal generator (PRSG). Then, the new image encryption algorithm is designed based on the proposed discrete system, and its safety performance is tested. The experimental results demonstrate the feasibility of its application in the field of cryptography.

INDEX TERMS Boosted control, extremely multistability, chaos enhancement, image encryption.

I. INTRODUCTION

Chaotic system has received a lot of attentions on account of its bright application prospects in the field of nonlinear engineering [1]–[6]. Generally speaking, extremely multistability shows that there are infinitely many numerical solution in the differential equations of a dynamical system with varying initial states [7], [8]. The original chaotic system of infinitely many equilibrium points or switchable equilibrium point has the ability to generate infinitely many coexisting attractors [9], [10]. Recently, another better method for constructing the system with extremely multistability was found, the initial-offset boosted attractors of infinitely many coexistence can be obtained by introducing the trigonometric functions to some specific linear terms of chaotic system [11]–[13]. The chaotic system which has infinitely many coexisting attractors depends extremely on the initial state. Thus, in comparison with some single stable

systems [14], [15], its dynamic behaviors are often more complex.

The initial-offset boosted multistability can provide more ergodicity and flexibility for some engineering applications based on chaos theory [16]. In particular, it can be applied to switch different dynamic states in the control of multistable state if combined with several suitable algorithms of control science [17]. Some recent studies show that a part of classic chaotic systems have the ability to generate coexisting attractors by their standalone attractor basins [18]–[20]. Classical 3D Lorenz system can produce two symmetric attractors from single attractor by adjusting the initial conditions [21]. Ye *et al.* found a new circuit system of extremely multistability by introducing a meminductive model to the 4D Wien-bridge oscillator [22]. In particular, some chaotic systems can generate extremely multistability by the boosted control of trigonometric function. Lai *et al.* obtained infinitely many coexisting attractors by introducing sine function to the Sprott B system [23]. The discovery of extremely multistable system was a leap from the finite to the infinite. Its potential

The associate editor coordinating the review of this manuscript and approving it for publication was Bing Li.

industrial application value is worth further and deeply exploring.

Third-order chaotic system is the lowest order continuous system which can generate the chaos attractor [24], it is the origin of research on continuous chaotic system. However, due to the lack of multiple feedback of the nonlinear term, 3D chaotic system is hard to spontaneously generate extremely multistability. Thus, constructing the extremely multistability based on 3D chaotic system is very crucial for chaotic basic demonstration teaching. This paper successfully constructed a new 3D chaotic system which can produce infinitely many coexisting attractors by using the boosted control of cosine function. Especially, due to the introduction of two cosine functions, it can generate two directions infinitely many coexisting attractors by changing different initial conditions. That means the proposed system can simultaneously output the pseudo-random signals of two directions in the phase plane. It greatly increased the chaos range and enhanced the pseudo-random performance of the chaos sequence. The proposed chaotic system has better chaos characteristic and higher sequence complexity, it provided a good model for the field of cryptography.

In this article, we focus on a new chaotic system of extremely multistability which can generate infinitely many coexisting attractors. It is organized as follows. In section 2, a new system model is proposed based on sprott system, and the equilibrium points is calculated. In section 3, Lyapunov exponents and Kaplan-Yorke dimension of the new system is calculated, its 3D chaotic attractor is presented. In section 4, the dynamic behavior of enhanced chaos in this proposed system is analyzed, and the complexity is compared. In section 5, the dynamic behavior of infinitely many coexisting attractors is analyzed. In section 6, the new encryption algorithm is designed, and its safety performance is tested. Finally, the proposed new system is successfully implemented by DSP.

II. CHAOTIC SYSTEM MODEL

A. SYSTEM EQUATIONS

The proposed system is a third-dimensional chaotic system of extremely multistability, and it originates from the reconstruction for a 3D chaos system proposed by Ref. [24]. The mathematical model of Ref. [24] is:

$$\begin{cases} \dot{x} = c(y - x), \\ \dot{y} = axz, \\ \dot{z} = b - xy, \end{cases} \quad (1)$$

where, x, y, z are state variables, and a, b, c are system parameter. This 3D system cannot generate coexisting attractors by itself standalone attractor basins. Then, reconstructing the system equation by introducing two boosted control of cosine function for state variables x, z , the chaotic system can generate infinitely many coexisting attractors of two directions on the phase plane. The mathematical equations of the proposed

system be expressed as:

$$\begin{cases} \dot{x} = y - \cos(2x), \\ \dot{y} = a \cos(2x) \cos(2z), \\ \dot{z} = b - \cos(2x)y, \end{cases} \quad (2)$$

in which, x, y, z are all state variables, and a, b are the positive constants. Parameter a can control the amplitude of chaotic sequence and b as a parameter of the nonlinear feedback loop. In order to reduce the period of cosine function, expand state variables x, z as $2x, 2z$. Its dynamic characteristics can be analyzed based on this chaotic system equations.

B. ANALYSIS OF DISSIPATION

If system (2) is a dissipation system, its condition is:

$$\nabla V = \frac{\partial \dot{x}}{\partial x} + \frac{\partial \dot{y}}{\partial y} + \frac{\partial \dot{z}}{\partial z} = 2 \sin 2x < 0. \quad (3)$$

Thus, when $x \in (k\pi + \pi/2, k\pi + \pi)$ ($k = 0, \pm 1, \pm 2, \dots$), the new system is considered to be dissipative. It indicates the running track of the system will compress to an empty set, and the progressive motion will tends to be stable in a domain of attraction.

C. EQUILIBRIUM POINTS SET

Let $\dot{x} = \dot{y} = \dot{z} = 0$, the equilibrium point of system (2) can be calculated:

$$S = [(x, y, z) | x = k\pi/4 + 0.5 \arccos(\sqrt{b}), y = \pm\sqrt{b}, z = k\pi/2 + \pi/4], \quad (4)$$

in which, $k = 0, \pm 1, \pm 2, \dots$, the Jacobian matrix at the equilibrium point S is:

$$J = \begin{bmatrix} 2 \sin(2x) & 1 & 0 \\ -2a \sin(2x) \cos(2z) & 0 & -2a \cos(2x) \sin(2z) \\ 2y \sin(2x) & -\cos(2x) & 0 \end{bmatrix}. \quad (5)$$

The third-order characteristic polynomial can be obtained:

$$P(\lambda) = \lambda^3 + k_1 \lambda^2 + k_2 \lambda + k_3 = 0. \quad (6)$$

Thus, we can calculate:

$$k_1 = \pm 2\sqrt{1-b}, k_2 = \pm 2ab, k_3 = 0 \text{ or } 8ab\sqrt{1-b}. \quad (7)$$

According to 3D Routh-Hurwitz stability criterion, we have the sufficient and necessary conditions for stability of the proposed new chaotic system is:

$$k_1 > 0, k_2 > 0, k_3 > 0, k_1 k_2 > k_3. \quad (8)$$

Because the equilibrium points of the proposed chaotic system are changed with the periodic change of the cosine function. An infinite number of attractors may be generated due to the extremely multistability of the chaos system.

III. ANALYSIS OF DYNAMIC BEHAVIOR

A. LYAPUNOV EXPONENTS AND KAPLAN-YORKE DIMENSION

The sensitivity to initial conditions is an important dynamical characteristic of chaos. It can cause a larger separation of two near orbits with varying initial state. These characteristics can be described by Lyapunov exponents, the positive Lyapunov exponent shows the instability of the phase orbitals, it indicates the system is chaos. The negative Lyapunov exponent shows the contraction of the running orbitals, it reflects the unstable points or periodic points. The attractors are formed from the repeated folding of chaotic orbits. The mathematical formula of a continuous system of differential equations be mathematically defined as:

$$\dot{Y}(t) = F[Y(t)], \tag{9}$$

where, $Y(t)$ is a function with varying time, $\dot{Y}(t)$ is a derivative of $Y(t)$, $F[Y(t)]$ means some functional relationship between two functions. Then, Eq. (9) can be treated by using Euler discretization method, and we have:

$$Y_{i+1} = Y_i + F(Y_i)\Delta t, \tag{10}$$

in which, $Y_i = Y(t)$, $Y_{i+1} = Y(t + \Delta t)$, Δt is a minute time variable. Define A^p are the p -order compound matrices of Jacobian matrix generated by $Y(t)$, then we have:

$$\tilde{A}^p(t) = K^p[Y(t)]A^p(t), \tag{11}$$

in the last formula, $A^p(t)$ is a p -order compound matrices on time variable. $K^p[Y(t)]$ is the limit value of the p -order compound matrices of Jacobian matrix within the range of time variable will approach to 0. Finally, we can get the computational formula of Lyapunov exponent of the continuous system:

$$\lambda = 1/t \lim_{t \rightarrow \infty} \ln \left| \frac{S^p(t)}{S^{p-1}(t)} \right|, \tag{12}$$

where, $S^p(t)$ is the trace of $\tilde{A}^p(t)$. The Lyapunov exponent value of the continuous chaos system can be calculated and obtained according to the above formula. Generally speaking, for a chaos system of n dimensions, the number of Lyapunov exponents are also n , the Lyapunov exponents λ_i ($i = 1, 2, \dots, n$) need satisfy the conditions $\lambda_1 > \lambda_2 > \dots > \lambda_n$. If it satisfies:

$$\begin{aligned} \lambda_1 + \lambda_2 + \dots + \lambda_j &> 0, \\ \lambda_1 + \lambda_2 + \dots + \lambda_j + \lambda_{j+1} &< 0, \end{aligned} \tag{13}$$

where, j is the max value of i which can satisfy the conditions $\sum \lambda_i > 0$, then we can obtain the Kaplan-Yorke dimension λ_L of Lyapunov exponent by the following formula:

$$\lambda_L = j - \sum_{i=1}^j \lambda_j / \lambda_{j+1}. \tag{14}$$

Setting system parameter $a = 15$, $b = 0.1$, the initial conditions of system. (2) $(x_0, y_0, z_0) = (0, 1, 0)$, The Lyapunov

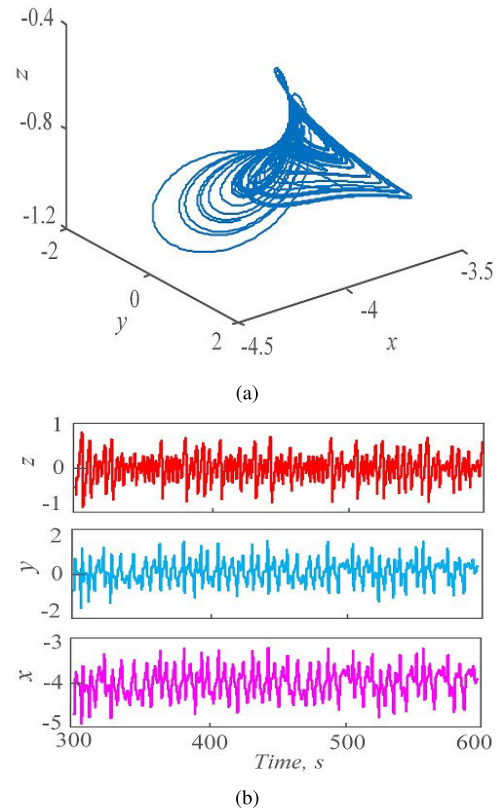


FIGURE 1. Chaotic attractors of the proposed system. (a) 3D chaotic attractors (b) The time sequence of length 300s~600s.

exponent values of the proposed chaotic system can be calculated by Eq. (9)-(12), they are $Ly_1 = 0.5045$, $Ly_2 \approx 0$, $Ly_3 = -1.7113$. Then we have the Kaplan-Yorke dimension of Lyapunov exponents $\lambda_L = 2.2948$, it means this system is chaos under this conditions. In comparison with the original system. (1), due to the new system is constructed by the boosted control of cosine function, it may have more complex dynamics characteristic in terms of Kaplan-Yorke dimension

B. CHAOS ATTRACTORS

Setting system parameter $a = 15$, $b = 0.1$, the initial conditions of system. (2) $(x_0, y_0, z_0) = (0, 1, 0)$. By using ODE45 algorithm, the chaotic attractors can be obtained by using numerical simulation. Fig. 1(a) shows the chaotic attractor in the 3D phase spaces. Obviously, the system is chaos in this case. To further explain the formation of attractors, the time sequences are analyzed and simulated. Let the time step is 0.01s and select the length 300s~600s as the object of study. The result of numerical simulation is represented in Fig. 1(b), it shows the system is in a stable chaotic orbits, and the attractors are formed by the superposition of their chaotic oscillations.

IV. ENHANCED CHAOS OF BOOSTED CONTROL

A. ENHANCED CHAOS IN THE DYNAMIC BEHAVIOR

Setting the initial value of system (1) $(x_0, y_0, z_0) = (0, 1, 0)$ and system parameter $c = 1$, $b = 0.01$. Parameter a is

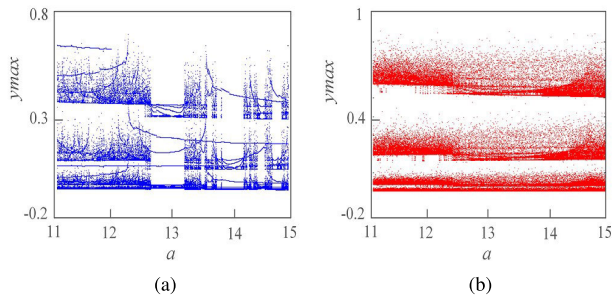


FIGURE 2. Enhanced chaos in the bifurcation diagram. (a) Bifurcation diagram of system (1) (b) Bifurcation diagram of the proposed chaos system.

the variable parameter, and the varying range is [11, 15]. As shown in Fig. 2(a), the bifurcation diagram of system (1) has a biggest periodic windows within $a \in [12.735, 13.226]$. Then, more periodic windows are generated as parameter a changes. When $a \in [13.833, 14.198]$, the system has another larger window. The generation of these periodic windows causes the system to produce intermittent chaotic oscillations. It has a negative effect on the industrial application of chaotic system. Let the initial state of the proposed system $(x_0, y_0, z_0) = (0, 1, 0)$ and system parameter $b = 0.01$. Parameter a as the variable parameter, and the varying range is also [11, 15]. (when system parameter of system (1) $a = 1$ and $c = 0.01$, the chaotic system of system (1) is equivalent to the proposed system without introducing two boosted control of cosine function) Fig. 2(b) shows the bifurcation diagram of the proposed chaotic system within the equivalent varying range of system (1). From the simulation result, most of periodic windows in Fig. 2(a) have become chaos due to the introduction of boosted control of cosine function. In comparison with system (1), the proposed chaotic system has almost no periodic windows within the test interval, and the chaotic state fills the whole range. That is to say, the chaotic behavior is enhanced. It greatly enhances the application of chaotic pseudo-random signals.

In order to further study the effect of system parameters on chaotic behavior. Keep the above parameters unchanged, select two system parameters a and b as the variable parameter, the varying range $a \in [11, 15]$ and $b \in [0, 1]$ respectively. With a and b synchronously changed, the max Lyapunov exponent of system (1) is shown in Fig. 3(a). When $a \in [11, 15]$ and $b \in [0.2, 0.4]$, system (1) has a bigger periodic windows. In particular, when $b \in [0.6, 1]$, the max Lyapunov exponents of system (1) all go down to 0, it indicates the system is in a periodic state, and the max value of the max Lyapunov exponent in this test range is 0.332. Fig. 3(b) shows the max Lyapunov exponent of the proposed chaos system. For comparative analysis, select the same varying range $a \in [11, 15]$ and $b \in [0, 1]$ as the test range. In comparison with system (1), the bigger periodic windows of $a \in [11, 15]$ and $b \in [0.2, 0.4]$ has disappeared, the max Lyapunov exponent value in this test range are within $0.5 \sim 1$. It shows the periodic

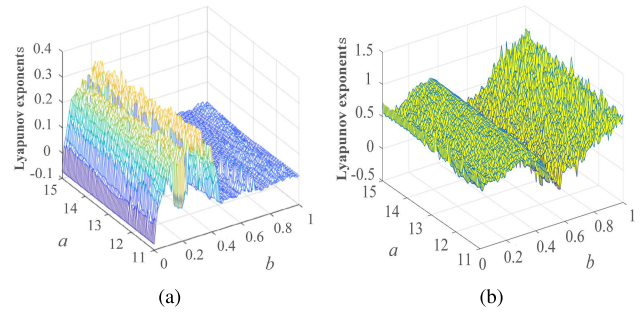


FIGURE 3. Enhanced chaos in Max Lyapunov exponents. (a) Max Lyapunov exponents of system (1) (b) Max Lyapunov exponents of the proposed chaos system.

windows in this range has become chaos state. The dynamic behaviors of system (1) is periodic in the range $b \in [0.6, 1]$. However, by introducing two boosted control of cosine function to state variables x, z , the max Lyapunov exponent of the proposed chaotic system has been improved significantly. In this test interval, the max value of the max Lyapunov exponent of the proposed chaotic system is 1.198. Relative to system (1), the chaos interval of the proposed chaos system has also been significantly increased, the chaotic property is enhanced.

B. ENHANCED CHAOS IN THE COMPLEXITY

The enhancement of dynamic behavior makes chaotic behavior transition from periodic state to chaotic state. In terms of the application of chaotic system, the complexity characteristic of chaotic sequences can more directly reflects the usability of a chaos system. Spectral Entropy (SE) complexity algorithm is a measure of a system based on Shannon entropy, it can effectively shows the complexity characteristic of chaotic system. The higher value of complexity reflects the stronger chaotic behavior generated by the chaos system. Spectral Entropy (SE) complexity algorithm can be described:

$$\tilde{x}(n) = x(n) - 1/n \sum_{i=1}^n x(i), \tag{15}$$

where, $x(n)$ is the energy amplitude of system. The function of Eq. (15) is to remove DC part of sequence. Then, do discrete Fourier transform, we have:

$$\tilde{X}(k) = \sum_{n=0}^{N-1} \tilde{x}(n)e^{-j\frac{2\pi}{N}nk}, \tag{16}$$

in which, $k = 0, 1, 2, \dots, N - 1$. Then, by using the Parseval theorem, we can calculate the relative power spectrum:

$$p(k) = \frac{1}{N} |X(k)|^2. \tag{17}$$

In Eq. (17), $k = 0, 1, 2, \dots, N/2 - 1$, and we have the total power:

$$\tilde{p} = \frac{1}{N} \sum_{k=0}^{N/2-1} |X(k)|^2. \tag{18}$$

Thus, the probability of power spectrum can be calculate, and we have:

$$\tilde{P}_k = \frac{p(k)}{\tilde{p}} = \frac{\frac{1}{N} |X(k)|^2}{\frac{1}{N} \sum_{k=0}^{N/2-1} |X(k)|^2}, \quad (19)$$

in which, N is the sequence length, $X(k)$ is the sequence after FFT. Combined with the above formula, we can obtain the computational formula of SE:

$$SE = -\ln(N/2) \sum_{k=0}^{N/2-1} P_k \ln \tilde{P}_k, \quad (20)$$

Based on the above formula, the spectral Entropy (SE) complexity of chaos sequence can be calculate, and the corresponding dynamic behavior can be analyzed.

C_0 complexity algorithm is also a complexity algorithm based on FFT. The proportion of irregular part between the regular and the irregular parts is C_0 complexity value. Its specific calculation method can be defined as:

$$\tilde{X}(k) = \sum_{n=0}^{N-1} \tilde{x}(n) e^{-j\frac{2\pi}{N}nk}, \quad (21)$$

where, $k = 0, 1, \dots, N - 1$, $\tilde{X}(k)$ is sequence the after FFT. Then, remove the regular part of sequence, we have:

$$\tilde{Y}(N) = \frac{1}{N} \sum_{k=0}^{N-1} |\tilde{X}(k)|^2, \quad (22)$$

in which, Y_N is mean square value. Then, if we introduce parameter r as a tolerance parameter, and reserve the mean square value which more than r , and other parts are zero, we have:

$$\hat{X}(k) = \begin{cases} \tilde{X}(k), & |\tilde{X}(k)|^2 > rY_N, \\ 0, & |\tilde{X}(k)|^2 < rY_N. \end{cases} \quad (23)$$

Then, do the inverse FFT, we can get:

$$\hat{x}(n) = 1/N \sum_{k=0}^{N-1} \hat{X}(k) e^{-j\frac{2\pi}{N}nk}. \quad (24)$$

where, $n = 0, 1, \dots, N - 1$. According to the above equations, C_0 complexity can be obtain:

$$C_0(r, N) = \sum_{n=0}^{N-1} |x(n) - \hat{x}(n)|. \quad (25)$$

In order to compare and analyze the above simulation results of bifurcation diagram and max Lyapunov exponent, keeping other parameters unchanged, select parameter a and b as the varying parameters, and the test ranges are also $a \in [11, 15]$ and $b \in [0, 1]$. Fig. 4(a) shows the SE (Spectral Entropy complexity) of system (1), with parameter a varying within $[11, 15]$ and b varying within $[0.2, 0.6]$, SE complexity value is larger in all test range, the max value is 0.513. However, with parameter b varying within $[0.6, 1]$, SE complexity value of system (1) falls instantaneously, even

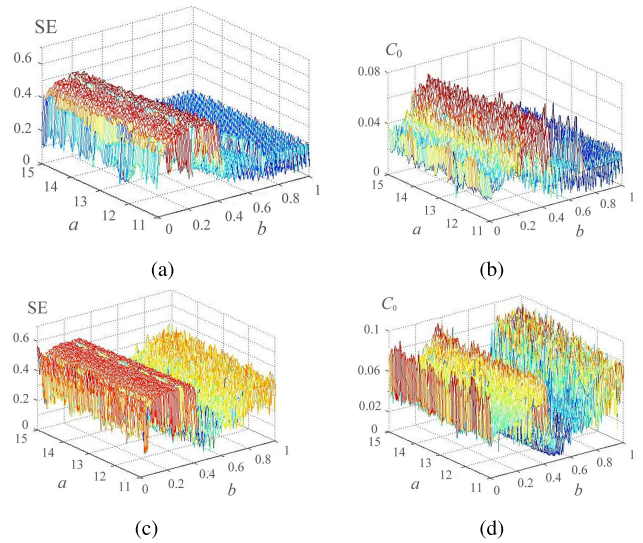


FIGURE 4. Enhanced chaos in complexity. (a) SE complexity of system (1) (b) C_0 complexity of system (1) (c) SE complexity of the proposed system (d) C_0 complexity of the proposed system.

to 0. It means the dynamic behavior of the system change state from a chaotic state to a periodic state. The corresponding simulation result of C_0 complexity is shown in Fig. 4(b). The max value of C_0 complexity is 0.075, and its varying trend is basically the same to its varying trend of SE complexity. SE and C_0 complexity of the proposed system can be shown in Fig. 4(c) and 4(d). From the simulation result, when parameter a varying within $[11, 15]$ and b varying within $[0.2, 0.6]$, the corresponding complexity spectrum become uniform and the complexity value has obviously gone up, the max value of SE complexity has already reached 0.581 and the max value of C_0 complexity is 0.093. The number of the periodic windows has been greatly reduced, and the complexity of the sequence has been greatly enhanced. By introducing two boosted control of cosine function, the periodic behavior has gradually changed into chaos when parameter $b \in [0.6, 1]$, the primary lower complexity value has also change into the higher complexity value. All of these have a positive impact on its industrial application.

V. INFINITELY MANY COEXISTING ATTRACTORS

Different initial conditions can generate different chaotic orbits after many periods of evolution. However, it is difficult for attractors to overstep the constraints of the attractor basin and form large changes in shape or phase. For a chaos system of extremely multistability, the differential equations has an infinite number of solutions. The shift of the equilibrium point causes a shift in the phase of the attractor. Fixed system parameters of the proposed system, select the initial conditions is $(x_0, 1, z_0)$, x_0 and z_0 are variables. When $a = 15$, $b = 0.4$, set the initial values are $(0, 1, 0)$, $(0, 1, \pi)$, $(0, 1, 2\pi)$, \dots , $(3\pi, 1, 3\pi)$, many coexisting attractors of periodic state are shown in Fig. 5(a). When $a = 15$, $b = 0.1$, and the initial values are $(0, 1, 0)$, \dots , $(3\pi, 1, 3\pi)$, many coexisting

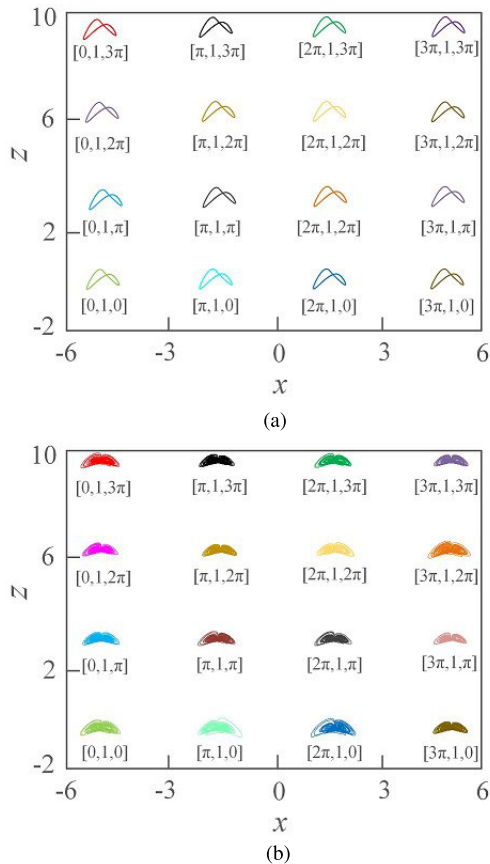


FIGURE 5. Many coexisting attractors. (a) Many coexisting attractors of periodic state (b) Many coexisting attractors of chaos state.

attractors of chaotic state are shown in Fig. 5(b). With two initial condition x_0 and z_0 varying simultaneously, the proposed system has extremely multistability. The phase position of attractors shifts periodically towards two directions of state variable x and z . It means this chaotic system can output chaotic signal with different amplitude at the same time. In comparison with system (1), the proposed chaos system can provide more ergodicity and flexibility for some engineering applications based on chaos theory.

VI. THE APPLICATION OF THE PROPOSED SYSTEM IN IMAGE ENCRYPTION

A. THE DISCRETE SYSTEM

Due to the chaos degradation problem caused by the finite precision, the random signal of the continuous chaotic system cannot be directly applied to digital encryption. Therefore, in order to make the proposed chaotic system better suitable for digital encryption applications, it can often be further discretized. In which, by using Gaussian discrete algorithm, the proposed continuous chaotic system can be effectively discretized. The specific discrete systems equation are shown as follows:

$$\begin{cases} x(n+1) = x(n) + h[y(n) - \cos(2x(n))], \\ y(n+1) = y(n) + h[a\cos(2x(n))\cos(2y(n))], \\ z(n+1) = z(n) + h[b - \cos(2x(n))y(n)], \end{cases} \quad (26)$$

where, a and b are control parameters, the step size h is set to 0.01 and n is number of cycles. Due to the characteristic of high pseudorandom, the chaos map is often used as a Pseudo Random Number Generator to generate the pseudo-random signal in engineering field.

B. CHAOTIC SECRET KEY

As shown in Fig. 6, a more than 300 bits-long secret key is applied in the design encryption algorithm. The design secret key is divided into 300 bits-long block S_1 and the secret key of initial value $x(0)$, $y(0)$, $z(0)$. Where, we set secret keys $x(0) = \pi$, $y(0) = 1$, $z(0) = \pi$. Then S_1 is divided into S_{11} , S_{12} , S_{13} , S_{14} , S_{15} , each of them can be divided into 60 bits-long. Especially in comparison with the single stable systems, the proposed new system of extremely multistability can generate infinitely many secret keys of initial value. This greatly increases the number of chaotic secret keys and thus increases the security of the encryption algorithm.

S (secret key)

| | | | | | | | |
|-----------------------------------|----------|----------|----------|----------|--------|--------|--------|
| S_1 (250bits) | | | | | $x(0)$ | $y(0)$ | $z(0)$ |
| S_{11} | S_{12} | S_{13} | S_{14} | S_{15} | | | |
| 60bit | 60bit | 60bit | 60bit | 60bit | | | |

FIGURE 6. The chaotic secret key.

C. THE DESIGN OF ENCRYPTION ALGORITHM

Based on the pseudo-random values generated by the proposed discrete chaos system, the diffusion formula of adjacent pixels can be constructed. As Eq. (27) shown, each pixel value of the design diffusion formula depends on the value of two adjacent pixels and the proposed discrete chaos system. Then, doing the xor diffusion operation between each pixel value of the second design diffusion formula and the value generated by the proposed discrete chaos system. Then, doing the scrambling operation between three first pixels and three last pixels.

$$\begin{cases} E_1(n+2) = \text{mod}[E_1(n+1) + \text{floor}(10^5 \times a \times (E_1(n) / 255) \times (1 - E_1(n)/255)) + P(n) + \text{floor}(x \times 10^{12}), 256], \\ E_2(n+1) = E_2(n) \oplus E_1(n) \oplus \text{mod}[\text{floor}(x \times 10^{12}), 256], \\ E_2(1) = E_2(\text{end}), E_2(2) = E_2(\text{end} - 1), \\ E_2(3) = E_2(\text{end} - 2), \end{cases} \quad (27)$$

in which, $p(n)$ is the pixel of the plaintext, $x(n)$ is the value generated by the proposed discrete chaos system, $E_1(n)$ is the pixel value of the first diffusion algorithm, and $E_2(n)$ is the pixel value of xor diffusion algorithm, and a is the control parameter of the proposed discrete chaos system. To further improve the anti-deciphering ability of the algorithm, the second diffusion algorithm is designed, and it can be

described as:

$$\begin{cases} EE(n+2) = \text{mod}[b \times \text{floor}((EE(n+1)/255) \times (1 - EE(n)/255)) + EE(n) + E_2(n) + \text{floor}(y \times 10^{12}), 256], \\ c_1 = \text{mod}[EE(1) + m_1 + \text{floor}(y \times 10^{12}), 256], \\ EE(1) = \text{mod}[c_1 + m_2 + \text{floor}(y \times 10^{12}), 256], \\ c_2 = \text{mod}[EE(2) + m_3 + \text{floor}(y \times 10^{12}), 256], \\ EE(2) = \text{mod}[c_2 + m_4 + \text{floor}(y \times 10^{12}), 256], \end{cases} \quad (28)$$

where b is the control parameter, $EE(n+2)$ depends on two adjacent pixels, $E_2(n)$ and the proposed discrete chaos system, c_1 and c_2 are the parameter which depend on the values of interference parameters m_1, m_2, m_3, m_4 . Then, do the third diffusion and scrambling operation:

$$\begin{cases} EEE(n+1) = EEE(n) \oplus EE(n) \oplus \text{mod}[\text{floor}(z \times 10^{12}), 256], \\ c_3 = \text{mod}[EEE(3) + m_1 + \text{floor}(z \times 10^{12}), 256], \\ EEE(3) = \text{mod}[c_3 + m_2 + \text{floor}(z \times 10^{12}), 256], \\ c_4 = \text{mod}[EEE(4) + m_3 + \text{floor}(z \times 10^{12}), 256], \\ EEE(4) = \text{mod}[c_4 + m_4 + \text{floor}(z \times 10^{12}), 256], \end{cases} \quad (29)$$

where $EEE(n+1)$ depends on the adjacent pixel $EEE(n)$, the pixel of last diffusion $EE(n)$ and the proposed discrete chaos system. Similarly, c_3, c_4 depend on the parameter m_1, m_2, m_3, m_4 and the value generated by the chaotic system. The images can be encrypted based on the design encryption formula, and the decryption algorithm is the inverse process of encryption algorithm.

D. THE ENCRYPTION AND DECRYPTION OF IMAGE

As Fig. 7 shown, based on the above proposed encryption algorithm, the plaintext image can be successfully encrypted and decrypted. In particular, the ciphertext image can effectively hide the core information of the original image. However, we cannot judge the performance of encryption only from the effect of ciphertext. The specific performance can be shown through the safety tests such as sensitivity of the secret key, histogram, information entropy and NPCR.

E. SENSITIVITY ANALYSIS OF THE SECRET KEY

Because the chaotic system is extremely sensitive to the initial state, extremely tiny variation of the initial secret key will generate a big difference after several iterations of the key sequence generator, and then the encryption effect can produce a big difference. It is because of this high sensitivity to initial values that chaotic systems are widely used in digital image encryption. In the design secret key, it is made up of 300 bits-long block S_1 and the secret key of initial values $x(0), y(0), z(0)$ and then we will do the sensitivity tests on them. Leave the other parameters unchanged, Fig. 8(a)-(c) show two ciphered Hill image only by changing the secret key of initial value $x(0)$ from π to $\pi + 10^{-14}$. Fig. 8(d)-(f) show two ciphered Hill image only by changing the secret key



FIGURE 7. The images of encryption and decryption. (a) Lena image of plaintext (b) Lena image of ciphertext (c) Lena image of decryption (d) Elaine image of plaintext (e) Elaine image of ciphertext (f) Elaine image of decryption (g) Hill image of plaintext (h) Hill image of ciphertext (i) Hill image of decryption.

of initial value $y(0)$ from 1 to $1 + 10^{-14}$. Fig. 8(g)-(i) show two ciphered Hill image only by changing the secret key of initial value $z(0)$ from π to $\pi + 10^{-14}$. The experimental results show the good security of the encryption algorithm based on the design chaos secret key.

F. THE ANALYSIS OF HISTOGRAM AND CORRELATION

Histogram is widely used in many applications of the computer vision. It can detect changes in a video by marking significant edge and color statistical changes between frames. Image histogram is a histogram used to represent the brightness distribution in a digital image, it plots the number of pixels of each brightness value in the image. The histogram is a statistical collection of data and distributes the statistical results into a set of predefined bins. From the experimental results of Fig. 9, the histograms of the plain images contain the key information, and the histograms of the ciphered images using the design algorithm is fairly flat distributed, it can effectively hide the key information of the image.

The correlation shows the strength between two adjacent pixels on the direction of horizontal, vertical and diagonal. It is one of most vital evaluation techniques in image encryption algorithm. The correlation coefficients test of Lena plain images and the ciphered images by using the proposed encryption algorithm are shown in Fig. 10. From the test result, the correlation of adjacent pixels in the plaintext image are higher, the concentration of the key information is high. However, the correlation of the ciphered image on the

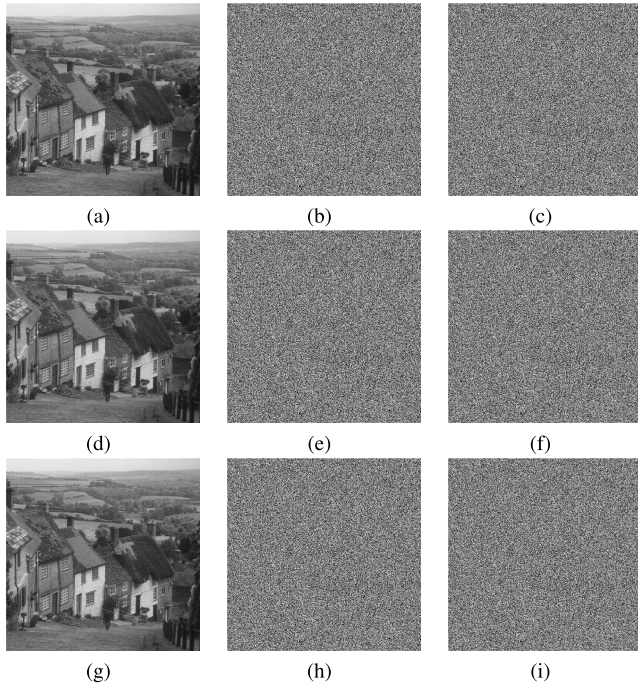


FIGURE 8. The sensitivity of the secret key. (a) Plaintext Hill (b) Original $x(0)$ (c) Changed $x(0)$ (d) Plaintext Hill (e) Original $y(0)$ (f) Changed $y(0)$ (g) Plaintext Hill (h) Original $z(0)$ (i) Changed $z(0)$.

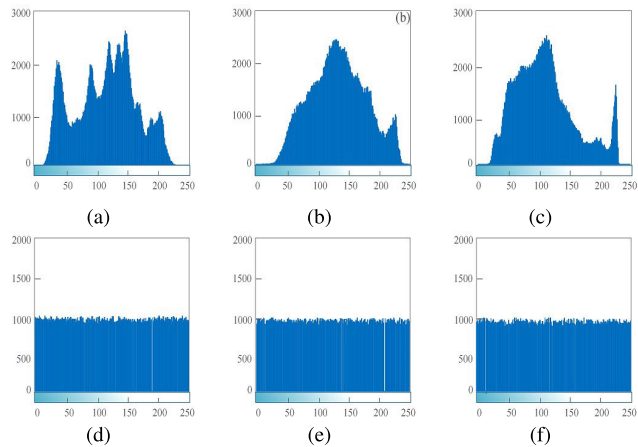


FIGURE 9. Histograms of images. (a) Histogram of Lena (b) Histogram of Elaine (c) Histogram of Hill (d) Histogram of ciphertext Lena (e) Histogram of ciphertext Elaine (f) Histogram of ciphertext Hill.

TABLE 1. Correlation coefficients of images.

| Image | Plain | | | Proposed | | |
|--------|------------|----------|----------|------------|-----------|-----------|
| | Horizontal | Vertical | Diagonal | Horizontal | Vertical | Diagonal |
| Lena | 0.972284 | 0.985612 | 0.959330 | 0.004933 | -0.002525 | 0.001991 |
| Elaine | 0.985497 | 0.983798 | 0.974217 | -0.004250 | -0.002352 | 0.003514 |
| Hill | 0.970982 | 0.974092 | 0.951980 | -0.001044 | 0.001023 | -0.002821 |

direction of horizontal, vertical and diagonal are all relatively low, even they are relevant. And the specific data of correlation coefficients test are shown in Tab. 1.

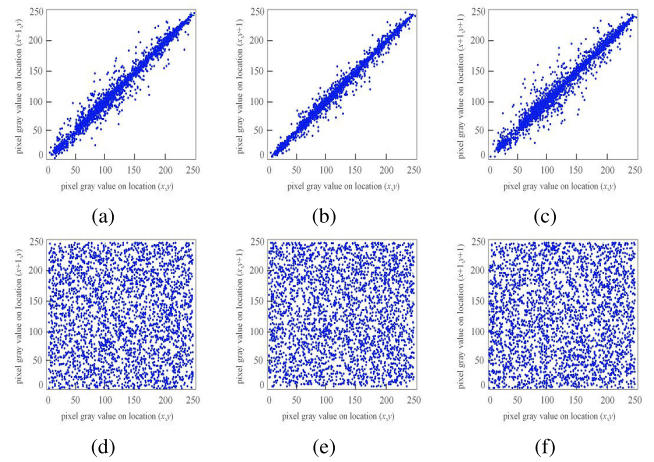


FIGURE 10. Correlation analysis of Lena image. (a) Horizontal correlation of the plain Lena image (b) Vertical correlation of the plain Lena image (c) Diagonal correlation of the plain Lena image (d) Horizontal correlation of the ciphered Lena image (e) Vertical correlation of the ciphered Lena image (f) Diagonal correlation of the ciphered Lena image.

G. ROBUSTNESS ANALYSIS

The ability to resist differential attack is often an important criterion to evaluate an algorithm. In general, tiny changes between adjacent pixels can cause major changes in image properties, NPCR (number of pixels change rate) and UACI (unified average changing intensity) are often used as a testing tool to measure this variation. The specific algorithm is described by:

$$\begin{cases} NPCR = \frac{\sum_{i,j} D(i,j)}{L} \times 100\% \\ UACI = \frac{1}{L} \sum_{i,j} \frac{|k_1(i,j) - k_2(i,j)|}{255} \times 100\%. \end{cases} \quad (30)$$

where k_1, k_2 are two encrypted images generated by two plain images with a pixel difference and its size is L . Generally, the ideal value of NPCR is 0.9961 and the ideal value of UACI is 0.3346. The closer the values of NPCR and UACI obtained from the design encryption algorithm are to the ideal values, the higher the safety performance. That is to say, the proposed algorithm has enough abilities to resist the differential attack. From the test results of NPCR and UACI in Tab. 2, the ability to resist differential attack of the design encryption algorithm is better.

The information entropy of image represents a chaotic degree of pixels, it represents the randomness and uncertainty of image information. It is also an important evaluation standard of the safety performance of encryption algorithm. The

TABLE 2. The test of UACI and NPCR.

| Algorithm | Lena | | Elaine | | Hill | |
|-----------|--------|--------|--------|--------|--------|--------|
| | NPCR | UACI | NPCR | UACI | NPCR | UACI |
| Proposed | 99.566 | 33.452 | 99.575 | 33.445 | 99.571 | 33.452 |
| Ref. [2] | 99.565 | 33.450 | 99.574 | 33.439 | 99.557 | 33.455 |
| Ref. [3] | 99.460 | 33.216 | - | - | 99.564 | 33.572 |

TABLE 3. Information entropy of the images.

| Algorithm | Lena | Elaine | Hill |
|-----------|----------|----------|----------|
| Plaintext | 7.446090 | 7.504811 | 7.476172 |
| Proposed | 7.999324 | 7.999221 | 7.999277 |
| Ref. [2] | 7.999322 | 7.999128 | 7.999317 |

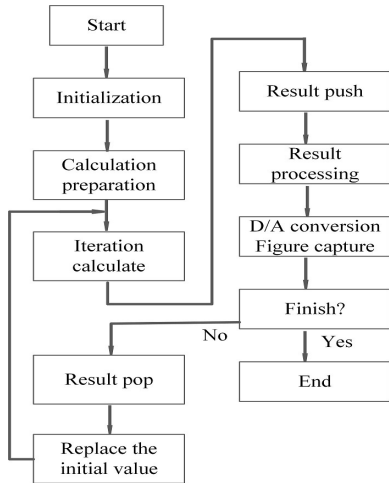


FIGURE 11. DSP implementation flowchart.

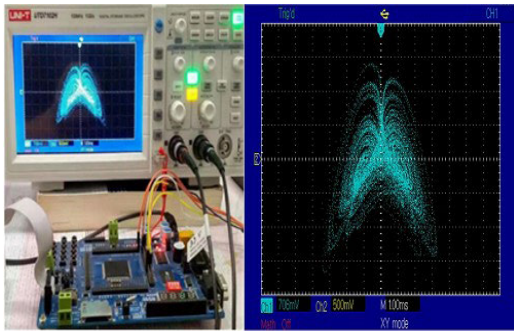


FIGURE 12. Chaotic attractor of DSP implementation.

specific formula can be described as:

$$H(k) = \sum_{i=0}^{2^N-i} p(k_i) \log_2 \frac{1}{p(k_i)}, \quad (31)$$

in which, $p(k_i)$ is the probability of k_i . The ideal value of information entropy is 8, the closer the value of information entropy obtained from the design encryption algorithm are to the ideal value, the better the safety performance. The information entropy of the proposed encryption algorithm is shown in Tab. 3. From the comparison result, the pixels have higher chaotic degree and anti-deciphering ability.

VII. DSP IMPLEMENTATION

To make the chaotic signal better suitable for digital chaos applications, the proposed system based on the boosted control of cosine function can be implemented by Digital Signal

Processing (DSP) technology. Select parameters $a = 15$, $b = 0.1$, and the starting condition $(0,1,0)$. According to the implementation flow as shown in Fig. 11, the chaotic attractors on $x-z$ plane can be digital implemented in Fig. 12. The experimental result of digital implement is basically the same to the analysis result of the numerical simulation, it shows the feasibility of theoretical analysis.

VIII. CONCLUSION

A new 3D chaotic system which can produce extremely multistability is reconstructed by the boosted control of cosine function. Base on its mathematical model, the Lyapunov exponents, Kaplan-Yorke dimension, bifurcation diagram and complexity can be simulated. In comparison with the original system, the proposed chaos system has better chaotic characteristic and higher complexity. Most of the cycle windows in the original chaos system became chaotic state, its chaos behavior was enhanced. Especially, the proposed system can generate infinitely many coexisting attractors due to the boosted control of cosine function. It means the proposed system can output more chaotic sequences of different amplitudes at the same time. These good performances have brought positive effects for its application in the industrial field. Next, we will continue to study the industrial applications based on this proposed chaotic system.

REFERENCES

- [1] X. Ye, X. Wang, S. Gao, J. Mou, Z. Wang, and F. Yang, "A new chaotic circuit with multiple memristors and its application in image encryption," *Nonlinear Dyn.*, vol. 99, no. 2, pp. 1489–1506, Jan. 2020.
- [2] X. Wang, H. Zhao, L. Feng, X. Ye, and H. Zhang, "High-sensitivity image encryption algorithm with random diffusion based on dynamic-coupled map lattices," *Opt. Lasers Eng.*, vol. 122, pp. 225–238, Nov. 2019.
- [3] A. Bakhshandeh and Z. Eslami, "An authenticated image encryption scheme based on chaotic maps and memory cellular automata," *Opt. Lasers Eng.*, vol. 51, no. 6, pp. 665–673, 2013.
- [4] F. Yang, J. Mou, H. Yan, and J. Hu, "Dynamical analysis of a novel complex chaotic system and application in image diffusion," *IEEE Access*, vol. 7, pp. 118188–118202, 2019.
- [5] F. Yang, J. Mou, K. Sun, Y. Cao, and J. Jin, "Color image compression-encryption algorithm based on fractional-order memristor chaotic circuit," *IEEE Access*, vol. 7, pp. 58751–58763, 2019.
- [6] X. Ye and X. Wang, "Characteristic analysis of a simple fractional-order chaotic system with infinitely many coexisting attractors and its DSP implementation," *Phys. Scripta*, vol. 95, no. 7, Jul. 2020, Art. no. 075212.
- [7] F. Yang, J. Mou, C. Ma, and Y. Cao, "Dynamic analysis of an improper fractional-order laser chaotic system and its image encryption application," *Opt. Lasers Eng.*, vol. 129, Jun. 2020, Art. no. 106031.
- [8] X. Ma, J. Mou, J. Liu, C. Ma, F. Yang, and X. Zhao, "A novel simple chaotic circuit based on memristor–memcapacitor," *Nonlinear Dyn.*, vol. 100, no. 3, pp. 2859–2876, May 2020.
- [9] C. Li, F. Min, Q. Jin, and H. Ma, "Extreme multistability analysis of memristor-based chaotic system and its application in image decryption," *AIP Adv.*, vol. 7, no. 12, Dec. 2017, Art. no. 125204.
- [10] C. Ma, J. Mou, P. Li, and T. Liu, "Dynamic analysis of a new two-dimensional map in three forms: Integer-order, fractional-order and improper fractional-order," *Eur. Phys. J. Special Topics*, vol. 230, nos. 7–8, pp. 1945–1957, Aug. 2021.
- [11] X. Li, J. Mou, L. Xiong, Z. Wang, and J. Xu, "Fractional-order double-ring erbium-doped fiber laser chaotic system and its application on image encryption," *Opt. Laser Technol.*, vol. 140, Aug. 2021, Art. no. 107074.

- [12] T. Liu, H. Yan, S. Banerjee, and J. Mou, "A fractional-order chaotic system with hidden attractor and self-excited attractor and its DSP implementation," *Chaos, Solitons Fractals*, vol. 145, Apr. 2021, Art. no. 110791.
- [13] N. Wang, G. Zhang, and H. Li, "Parametric control for multi-scroll attractor generation via nested sine-PWL function," *IEEE Trans. Circuits Syst. II, Exp. Briefs*, vol. 68, no. 3, pp. 1033–1037, Mar. 2021.
- [14] V. N. Giap, Q. D. Nguyen, and S. C. Huang, "Synthetic adaptive fuzzy disturbance observer and sliding-mode control for chaos-based secure communication systems," *IEEE Access*, vol. 9, pp. 23907–23928, 2021, doi: [10.1109/ACCESS.2021.3056413](https://doi.org/10.1109/ACCESS.2021.3056413).
- [15] T. Liu, S. Banerjee, H. Yan, and J. Mou, "Dynamical analysis of the improper fractional-order 2D-SCLMM and its DSP implementation," *Eur. Phys. J. Plus*, vol. 136, no. 5, p. 506, May 2021.
- [16] C. Li, Y. Peng, Z. Tao, J. C. Sprott, and S. Jafari, "Coexisting infinite equilibria and chaos," *Int. J. Bifurcation Chaos*, vol. 31, no. 5, Apr. 2021, Art. no. 2130014.
- [17] C. Li, J. Sun, J. C. Sprott, and T. Lei, "Hidden attractors with conditional symmetry," *Int. J. Bifurcation Chaos*, vol. 30, no. 14, Nov. 2020, Art. no. 2030042.
- [18] Q. Lai, Z. Wan, P. D. K. Kuate, and H. Fotsin, "Dynamical analysis, circuit implementation and synchronization of a new memristive hyperchaotic system with coexisting attractors," *Modern Phys. Lett. B*, vol. 35, no. 10, Apr. 2021, Art. no. 2150187.
- [19] H. Bao, Z. Hua, N. Wang, L. Zhu, M. Chen, and B. Bao, "Initials-boosted coexisting chaos in a 2-D sine map and its hardware implementation," *IEEE Trans. Ind. Informat.*, vol. 17, no. 2, pp. 1132–1140, Feb. 2021.
- [20] H. Bao, M. Chen, H. Wu, and B. Bao, "Memristor initial-boosted coexisting plane bifurcations and its extreme multi-stability reconstitution in two-memristor-based dynamical system," *Sci. China Technol. Sci.*, vol. 63, no. 4, pp. 603–613, Apr. 2020.
- [21] C. Li, J. C. Sprott, and H. Xing, "Hypogenetic chaotic jerk flows," *Phys. Lett. A*, vol. 380, nos. 11–12, pp. 1172–1177, 2016.
- [22] X. Ye, X. Wang, H. Zhao, H. Gao, and M. Zhang, "Extreme multistability in a new hyperchaotic meminductive circuit and its circuit implementation," *Eur. Phys. J. Plus*, vol. 134, no. 5, p. 206, May 2019.
- [23] Q. Lai, P. D. K. Kuate, F. Liu, and H. H.-C. Iu, "An extremely simple chaotic system with infinitely many coexisting attractors," *IEEE Trans. Circuits Syst. II, Exp. Briefs*, vol. 67, no. 6, pp. 1129–1133, Jun. 2020.
- [24] J. C. Sprott, "Some simple chaotic flows," *Phys. Rev. E, Stat. Phys. Plasmas Fluids Relat. Interdiscip. Top.*, vol. 50, no. 2, pp. 647–650, 1994.



BING LIU received the B.S. degree in mathematics from Liaoning Normal University, Liaoning, China, in 1992, the M.S. degree from the Faculty of Science, Northeastern University, Liaoning, in 1998, and the Ph.D. degree in mathematics and systems science from the Chinese Academy of Sciences, Beijing, China, in 2004.

From 2004 to 2006, she was a Postdoctoral Fellow with Xinjiang University, Xinjiang, China. From 2008 to 2009, she was a Senior Visiting

Scholar with the University of Liverpool, England. She has published more than 34 SCI papers and successfully selected as the 2010 Liaoning Provincial Higher Education Excellent Talents Support Program. She has achieved academic achievements of high academic level and application value. Her research interests include biological resource management, integrated pest management, and population model under environmental pollution.



XIAOLIN YE (Graduate Student Member, IEEE) received the B.Sc. and M.Sc. degrees in communication engineering and control science and engineering from Dalian Polytechnic University, China, in 2010 and 2018, respectively. He is currently pursuing the Ph.D. degree in computer application technology with Dalian Maritime University, China.

His research interests include nonlinear circuits and systems and image encryption technology based on chaos.



QIANQIAN CHEN received the B.Sc. degree in communication engineering from Dalian Polytechnic University, China, in 2009, and the B.Sc. degree in automation engineering from Dalian University of Technology, China, in 2012. Her research interests include nonlinear sciences and deep learning.

...